

TCMS: A Software for Vibration-Based Condition Monitoring of Post-Tensioned External Tendons

Milad Cheraghzade¹, Mohsen Ghafory Ashtiany^{2*}, and Omid Bahar³

1. M.Sc. Student, Structural Engineering Research Center, International Institute of Earthquake Engineering and Seismology (IIEES), Tehran, Iran
2. Professor, Engineering Department, Structural Engineering Research Center, International Institute of Earthquake Engineering and Seismology (IIEES), Tehran, Iran,
*Corresponding Author; email: ashtiany@iiees.ac.ir
3. Associate Professor, Structural Engineering Research Center, International Institute of Earthquake Engineering and Seismology (IIEES), Tehran, Iran

Received: 05/04/2021

Accepted: 11/07/2021

ABSTRACT

This paper presents a developing open-source software, named TCMS (Tendon Condition Monitoring Software), for condition monitoring of post-tensioned external tendons. This software allows users to run a complete process with three main goals: pre-processing of the input data, system identification for modal analysis, and tensile force estimation. A new Graphical User Interface (GUI) designing tool, App-Designer, is used to create a friendly GUI on the MATLAB software environment of MathWorks. A new approach for Finite Element (FE) modeling of an experimental tendon in which the load-bearing component is separately developed from the mass and stiffness components is also presented. The FE tendon model's modal parameters are identified from modal analysis to validate the applicability of TCMS. Then, the identified mode shape ratios and frequencies are used for vibration-based tensile force estimation. A comparative study based on provided tools and FE models in TCMS is conducted on different methods for tensile force estimation. The obtained results show that the existing tensile force using different methods can be estimated with accuracy in an average range of 1 to 10%. The current version of TCMS is mainly focusing on the establishment of examined modules for tensile force estimation. The TCMS source-code and data are available online on: <https://github.com/miladcheraghzade/TCMSSoftware.git>.

Keywords:
MATLAB;
App-Designer;
Condition monitoring;
Tendon; Tensile force
estimation; Vibrational
measurement

1. Introduction

Tensile force estimation of axially one-dimensional tensioned members in different structure types, including stay cables in cable-stayed bridges, suspensions in arch bridges, and post-tensioned tendons in box girder concrete bridges, have a significant role in the health monitoring of the entire structure. These load-bearing components take up a high percentage of construction costs. Early distress assessment

methods can be implemented to evolve the structure's service period equipped with these components. Some approaches have been adopted in engineering practice for tension estimation in the in-service stage and during construction. Direct measurement, load cells, or strain gages have been used for tension estimation, but high cost, lack of accuracy, and damage potential restricted all these methods applicability. Optical

fiber Bragg grating sensors (OF-BGS) have been used to monitor the stresses in bridge stay cables by embedding inside the cross-section to measure the corresponding strain and then changes in cable forces [1]. The magnetoelastic method has also been used for tension estimation; however, the associated problems with installing and manipulating the test restrict its flexibility [2].

Vibration-based measurement methods have been extensively used for tensile force estimation as a popular and promising approach. The technical development of vibration-based measurement methods allows one to implement them with more simplicity. However, the required algorithm and tools are well examined. Accordingly, the TCMS (Tendon Condition Monitoring Software) is developing, focusing on vibration-based methods.

Two different approaches have been used in engineering practice for System Identification (SI) of civil engineering structures. Forced vibration and ambient vibration have been widely performed to excite the systems, where their dynamic characteristics can be sensed and extracted as vibrational responses. Mathematical algorithms are used to extract system features with lower dimensions, such as modal features (i.e., modal frequencies and shapes). BRIMOS (Bridge Monitoring System) has been successfully used to this aim, implementing different mathematical algorithms, including Peak-Picking (PP) and Stochastic Subspace Identification (SSI) [3].

Ambient vibration at the earlier stage has been used by determining the natural frequencies of stay cables. The identified frequencies have been used to input the pre-determined analytical formula in String theory for tensile force estimation [4]. Sag effects, flexural stiffness, complicated boundary conditions that are not considered in String theory result in questionable accuracy for tensile force estimation [5-6]. In more recent works, the effect of flexural stiffness is considered using Beam theory as a beam subjected to axial load. A practical formula has also been driven with an expression that covers both String and Beam's theory [7]. Moreover, different boundary conditions are also considered

for tensile force estimation. Sagüés et al. [8-10] conducted a forced vibration method for tensile force estimation of external post-tensioned tendons using Beam theory, where they used a dead blow hammer to excite the tendons and recorded the acceleration response of the tendon.

At the beginning of implementing the Beam theory for tensile force estimation, the researchers considered Beam's theory with a hinged-hinged boundary condition at both ends. Then they concluded that the clamped-clamped boundary condition shows more accurate results for tensile force estimation of tendons [8-10]. Also, Different damage effects on tendon grout and load-carrying members using vibrational responses have been investigated for different experimental tendon specimens [11].

All the above formulas for String and Beam's theory have an ambiguous state for different types of cables with different boundary and geometrical conditions. Therefore, a comprehensive field study has also been conducted for all available vibration-based tension estimation techniques by classifying the relationship between frequencies and tension [12]. In addition, a novel method has been thoroughly explored using mode shape functions determined from multiple measurements. Multiple measurements on different cable locations and determining the mode shape ratios effectively tackled the parameter issues associated with pre-determined formulas, where this method is successfully applied to different cable types, including stay cables of Chi-Lu Bridge [13], tendons in segmental box girder bridges [14], suspensions in arch bridges [15], and the method has been extensively explored to establish a mathematical foundation by means of sensor deployment in engineering applications [16].

To better observe and control data quality through data analysis procedures and make the built-in functions interactive between the user and computer, the TCMS is provided with an interface using MATLAB's App-Designer front-end programming tool. MATLAB already has front-end programming tools as the code base and GUIDE Environment programming. Nevertheless,

since the 2017 versions, it has been provided with App-Designer, which has more advantages over the preceding tools. For example, multiple tabs, trees, and various knobs are added with the object-oriented nature of its script coding. Moreover, the users are able to execute their product as a stand-alone or web-based version.

A stand-alone software named TCMS is introduced for condition monitoring of post-tensioned external tendons on the MATLAB platform. Despite all the conducted research, a comprehensive and integrated tool is required to bring pre-examined methods for tensile force estimation together. Prerequisite algorithms for pre-processing data, SI, and curve fitting are also required through the tensile force estimation process. With open-source code and data of TCMS, various accesses to different software, which is mostly commercial, is not required. TCMS brings all the mentioned methods and algorithms together, where the sensitivity of the analysis process can be assessed with different assumptions and methods based on developed tools for comparison. A comparative study is also conducted to evaluate the accuracy and simplicity of different methods for tensile force estimation embedded in the software. A proposed FE modeling approach is introduced to achieve a better-simulated model, and in addition, a new post-tensioning approach is also implemented on the proposed model. First, different approaches and algorithms embedded in the software are also explained in summary to make the manuscript stand alone. Then, an overview of the software and methodology in all mentioned parts is given. Finally, the usefulness of the TCMS is validated with different FE model examples with a user-friendly interface where the data analysis can be done with great ease.

2. Methodology and Overview

The TCMS's different internal modules are grouped into four primary tabs with some nested tabs. Thus, different embedded algorithms based on their different functionality, as core functions, can be implemented to control the data processing procedure. All the tab groups are as follows, with

a schematic workflow of which is given in Figure (1).

- Filter parameters;
- Data correction (filter and baseline);
- System Identification (Peak-Picking);
- Preliminary frequency detection;
- Tensile force estimation;
- Saving data and report generation.

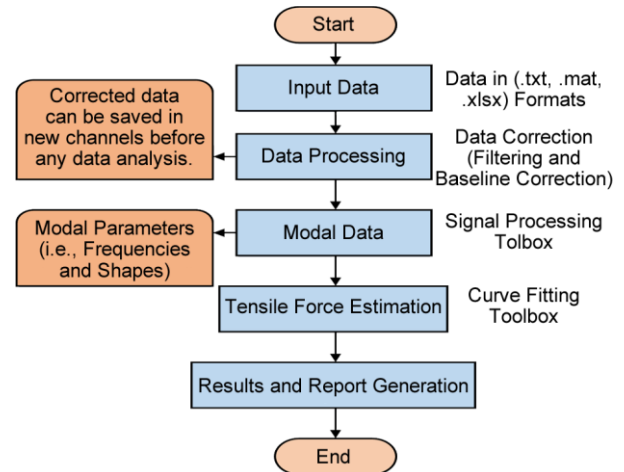


Figure 1. General workflow of TCMS.

Despite all well-documented programming languages like Python with its powerful libraries (i.e., NumPy, SciPy) for numerical computation, the MATLAB software package offers a wide variety of toolboxes with high functionality and easy accessibility. For example, TCMS embedded algorithms (e.g., PP and mode shape determination algorithms) needed for tensile force estimation are mostly available on commercial software like ARTEMIS for modal analysis. However, the most important advantage of TCMS is that it allows users to have free access to these algorithms, mostly available on commercial software.

Various modules are developed to conduct data pre-processing, modal analysis and extracting modal responses, and tensile force estimation. Different FE models simulated based on experimental data are developed to be used for the validation of TCMS. A new modeling approach of the tendon is developed to achieve better simulation accuracy. The mass and stiffness components and load-bearing components are separately modeled. The load-bearing component

is modeled as a wire section embedded inside a solid 3D model with tight interaction. Finally, the results of different methods obtained from different models are compared as a comparative study based on the different methods for tensile force estimation. The software mainly aims to be used by inspectors where only background knowledge about data cleaning and correction, frequency extraction and system identification, sensor deployment, and regression is required. The first version can be considered for elementary engineering and research purposes; however, the software's main objective for monitoring tendons for force estimation is covered.

Different sections of this article are as follows: A background is given on the embedded algorithms in TCMS in Section 3, applications of TCMS and numerical modeling are presented in Section 4, the results of tensile force estimation based on the previous sections are presented in Section 5, and finally, the developed GUI is presented in appendix A.

3. Theoretical Background

In this section, a summary is given on different algorithms embedded in TCMS. The theoretical background of algorithms coded as core functions is summarized in four sub-sections as follows.

3.1. Data Correction

Almost all the building environment structures are subjected to ambient noise due to human activities, wind, and atmospheric phenomena. While capturing the system's responses, one must pay attention to these ambient noises, resulting in false system identification. Butterworth filtering is used for data cleaning to remove the effects of these background noises in this software. Butterworth is an analog filter with smooth gain curves, which are often used [17]. Four Butterworth filters, such as Low Pass, High Pass, Band Pass, and Band Stop filtering are embedded in the software [18]. The filter parameters can be selected, and the different parameter effects can be observed with the procedure, as shown in Figure (2).

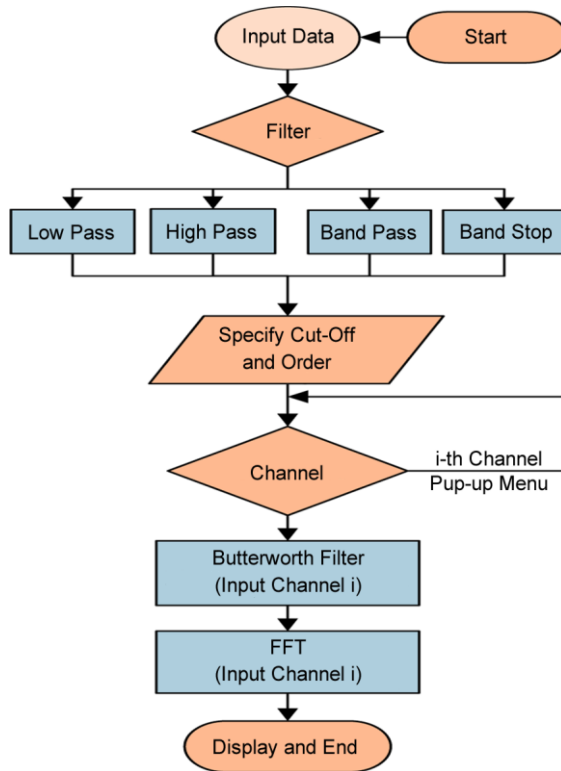


Figure 2. Flowchart showing the steps of the filter parameters selection.

Besides, all ambient noises that affect the structural system's captured data, some error also exists associated with data acquisition equipment or methods that need to be removed. For example, baseline errors in signal waveform affect the mode shape ratios. Therefore, to have a well-distributed mode shape over tendon length used in the mode shape function method, this error must be cleared. These errors exist in both analog and digitally recorded data. Chiu [19] in 1997 declared that most baseline errors consist of constant drift in acceleration, low-frequency noise in instrument noise, low-frequency background noise, and small initial values in acceleration and velocity. In TCMS, the algorithm tested by Chiu as three steps, including fitting the baseline of acceleration, applying a high pass filter in acceleration, and subtracting the initial values in velocity, is embedded as a built-in function for baseline correction. The data correction procedure is shown in Figure (3).

3.2. System Identification

The inputs for the tensile force estimation procedure are the extracted natural frequencies.

The coefficients of fit function for the relationship between mode order and frequencies are used for tensile force estimation in String and Beam theory as pre-determined formulas. Different steps for determining the natural frequencies extracted from raw data of different synchronized sensors are presented in Figure (4).

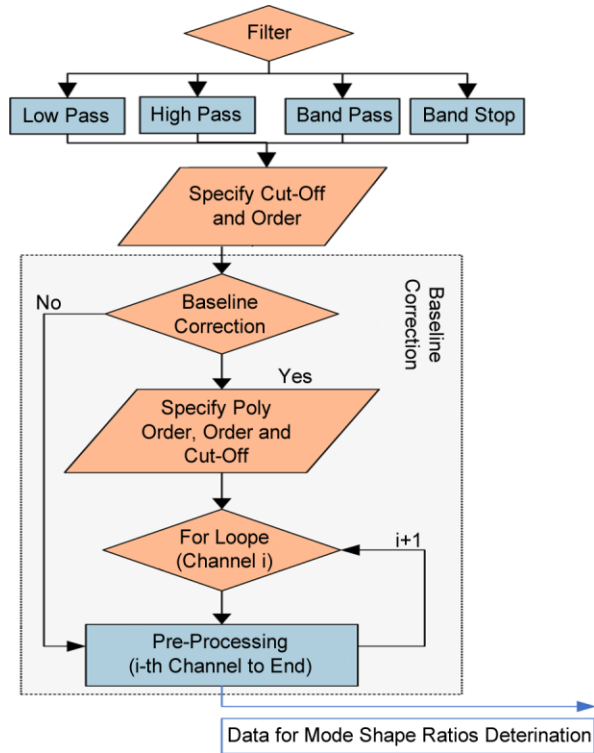


Figure 3. Flowchart showing the steps of the data correction.

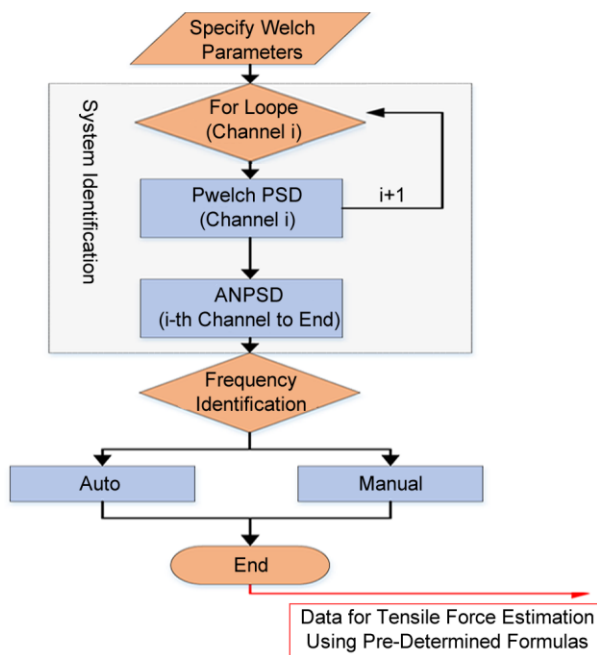


Figure 4. Flowchart showing the steps of the System Identification procedure.

Traditional Fourier transform is a mathematical algorithm to transform a signal from the time domain into the frequency domain as weighted combinations of sinusoidal basis functions. This transform led naturally to the concept of the spectrum where frequencies can be observed as peak values of the Power Spectral Densities (PSDs). Modal frequencies of tendons as one-dimensional members with flexural rigidity can be identified by mounting sensors (i.e., displacement, velocity, and acceleration sensors) on their length. The mounted sensors may be located at positions near the blind zone or node of vibration modes. Therefore, to better identify all the natural frequencies, a combination of all PSDs together can be used as Average Normalized Power Spectral Densities (ANPSDs) [20]. The average normalized PSDs equation is as follows:

$$ANPSD(f_k) = \frac{1}{l} \sum_{i=1}^{i=l} \frac{PSD_i(f_k)}{\sum_{k=0}^{k=n} PSD_i(f_k)} \quad (1)$$

where f_k is discrete frequency, and n is the number of discrete frequencies. With a time average of over windowed periodograms, the Welch algorithm is used to determine the PSDs for each data channel [21].

3.3. Tensile Force Estimation

In the earlier works, accurate estimation of parameters in the vibration equation of cable was the subject of some researches as parameter issues. Among all the parameters associated with the vibration equation, including mass per unit length and flexural rigidity, determining effective vibrational length is essential for proper tensile force estimation.

In this research, the accuracy of tensile force estimation with the anchorage-to-anchorage length of tendons using vibrational pre-determined formulas (i.e., String and Beam theory) is compared with the mode shape functions method.

Cables have slight bending stiffness; however, for the sake of simplification, this stiffness was not considered for tensile force estimation as String's theory in Equation (2). The tensile force

and mass are only considered in driving the String theory. However, the tensile force estimation results have questionable accuracy without considering the stiffness effect due to the anchorage, grout, and stiff duct on determining frequencies. In the most recent works, this stiffness was considered as Beam's theory with hinged-hinged boundary conditions in Equation (3) and clamped-clamped in Equation (4) [22].

$$f_{k_s} = \frac{k}{2l} \left(\frac{N}{m} \right)^{\frac{1}{2}} \quad (2)$$

$$f_k = \frac{k}{2l} \left(\frac{N}{m} \right)^{\frac{1}{2}} \left[1 + \left(\frac{k\pi}{\zeta} \right)^2 \right]^{\frac{1}{2}} \quad (3)$$

$$f_k = \frac{k}{2l} \left(\frac{N}{m} \right)^{\frac{1}{2}} \left[1 + \frac{2}{\zeta} + \left(4 + \frac{k^2 \pi^2}{2} \right) \frac{1}{\zeta^2} \right] \quad (4)$$

With

$$\zeta = l \left(\frac{N}{EI} \right)^{\frac{1}{2}}$$

where f_k and f_{k_s} signify the natural frequency of k-th mode, N is axial tension, EI is flexural stiffness, m is mass per unit length, l is the considered length, and ζ related bending stiffness. For tensile force estimation in all the above formulas determining the frequency of some modes is needed. Then a classic regression is needed to determine N in Equation (2), N , and EI in Equation (3) or Equation (4), as shown in Figures (5a) and (5b). Frequency determination can be done through different SI algorithms (e.g., FFT, PP., and SSI). In the TCMS, the PP algorithm is used for system identification, as explained in Section 3.2. It needs to be noted that the variables in the clamped-clamped beam formula as Equation (4) are not independent. Therefore, N and EI values have to be obtained by minimizing the differences between measured and calculated frequencies through an optimization procedure, as shown in Figure (5c) [23].

$$\left(\frac{f_k}{k} \right)^2 = \frac{N + \frac{k^2 \pi^2 EI}{l^2}}{4ml^2} \quad (5)$$

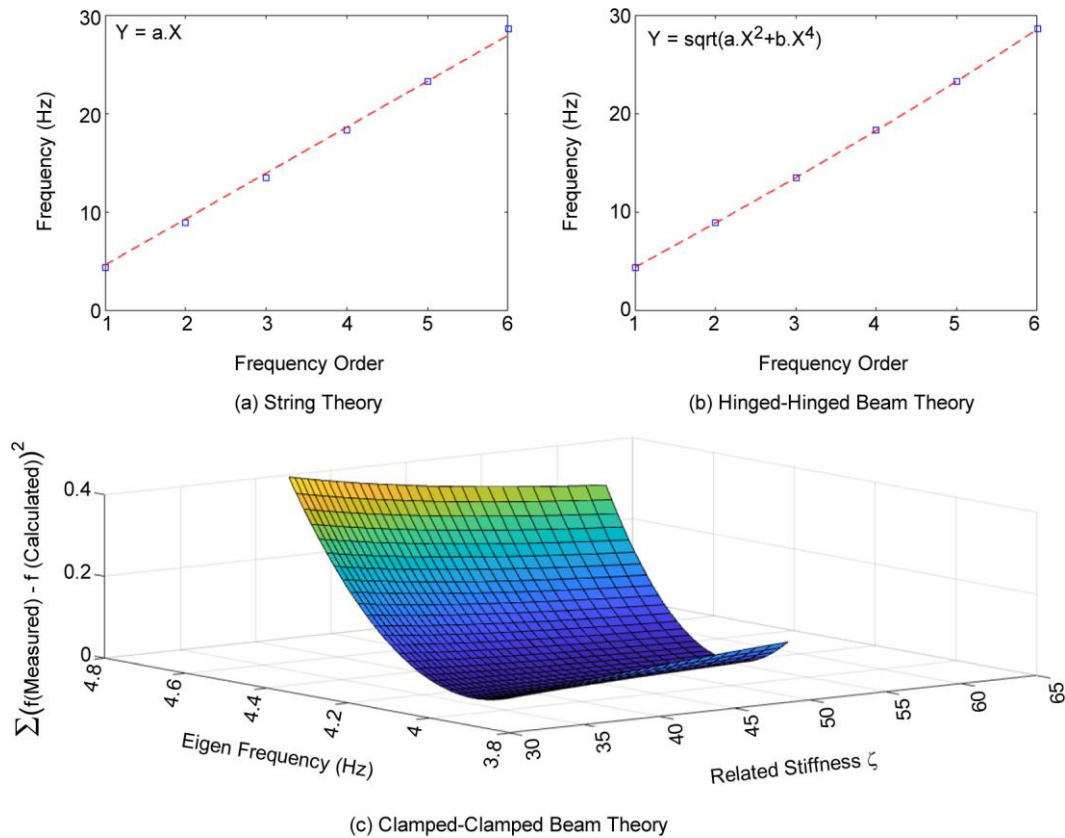


Figure 5. The objective functions for regression.

In Equation (5) that is a simplified form of Equation (3), three parameters appear for regression: N , EI , and l . Therefore, the tensile force and EI values can be obtained from a non-linear regression if only the modal frequencies are available.

As a novel method for further examination, the effective vibrational length can be obtained with mode shape functions and identified frequencies [13]. Therefore, the regression with an objective function as Equation (5) becomes a linear regression with two variables as N and EI . Furthermore, each location of the tendon has a certain displacement in each mode of vibration. Therefore, the mode amplitudes for each frequency can be estimated by recording the dynamic tendon responses on defined vibrational mode locations.

It is then possible to determine the tendon response phase from its FFT spectrum complex sign, and accurate mode shape ratios can be determined from the data obtained. For determining boundary point locations, the origin point coordinate has been transported to the mid-length of the cable, where the sensor's location fall in the range between $-l/2 < x < l/2$ instead of $0 < x < l$. Thus, the odd mode shapes turn to cosine, and the even mode shapes turn to sinusoidal functions as Equation (6), where the a_k is the amplitude of k-th mode.

$$\varnothing_k = a_k \begin{cases} \cos \frac{k \pi x_1}{l} \\ \sin \frac{k \pi x_2}{l} \\ \vdots \\ \cos \frac{k \pi x_m}{l} \end{cases} \quad k = k_1, k_2, k_3, \dots, k_m \quad (6)$$

The objective function for optimization has been declared with two parameters as a_k and l , in Equation (7). Furthermore, this is a non-linear optimization problem where the non-linear least-square algorithm (LS) is used for solving the optimization problem, starting from any initial values.

$$Error = \sum_{k=k_1}^{k_m} \sum_{j=1}^n (\varnothing_{ik} - \hat{\varnothing}_{jk})^2 = \sum_{k=k_1}^{k_m} \sum_{j=1}^n \left[a_k \cos \left(\frac{k \pi x_j}{l} \right) - \hat{\varnothing}_{jk} \right]^2 \quad (7)$$

where \varnothing_{ik} is the mode shape ratio vector of k-th mode. Different steps for tensile force estimation using both discussed methods can be thoroughly evaluated, as shown in Figures (6) and (7).

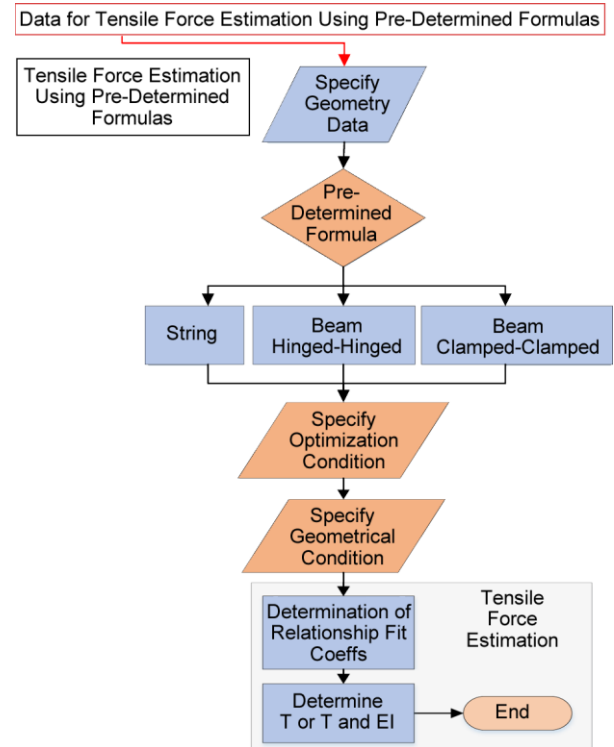


Figure 6. Flowchart showing the steps for tensile force estimation using pre-determined formulas.

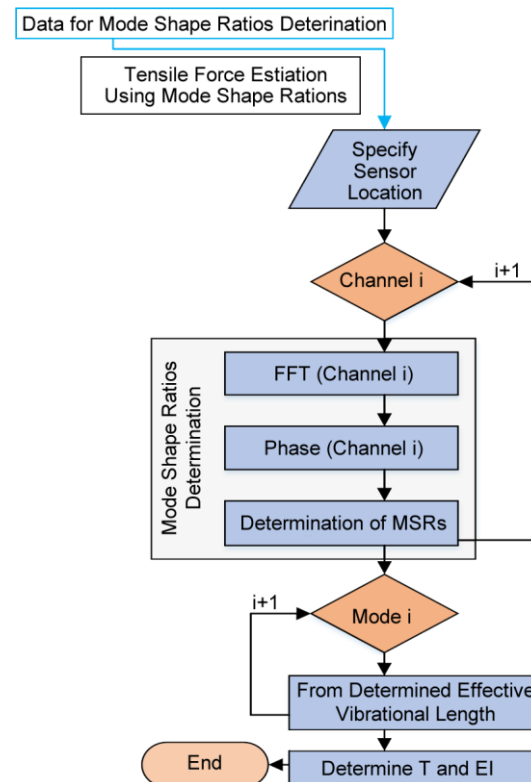


Figure 7. Flowchart showing the steps of tensile force estimation using mode shape functions method.

3.4. Pre-Determined Formulas (Method-1)

From identified frequencies using PP algorithm as explained in Section 3, and mode orders, the relationship between tensile force and identified frequencies could be determined with best-fit coefficients determined from the LS algorithm for any initial values. The fit function coefficients depend on the pre-determined formulas as objective functions, as explained in Section 3.3.

3.5. Mode Shape Functions (Method-2)

As explained in Section 3.3, the vibrational length of each mode can be determined using mode shape ratio vectors. However, the tendon mode shape includes two different hyperbolic and sinusoidal components, where the sinusoidal component is dominated [16]. Therefore, to determine the effective vibrational length for each mode of the tendon, the hyperbolic component is neglected.

This tab is developed to explore the mode shape function method for tensile force estimation. The user can use this method with multiple sensors from multiple measurements. TCMS allows the user to use up to 10 sensors for determining mode shape ratios with corresponding sensor positions. The Mode Shape Ratio (MSR) function is embedded in TCMS, adopting FFT amplitudes times their phase values to determine the mode shape vector as Equation (8).

$$MSR_n = \sum_{i=1}^n T_f \cdot \varnothing_f \quad (8)$$

where T_f represent the transfer function's amplitude at f , \varnothing_f represents the phase values at f , and n is the sensor number. With the identified mode shape ratios, the effective vibrational length is determined as the best cosine and sinusoidal functions fitted to the mode shape ratio vectors as Equation (6) and Equation (7).

4. Practical Application

This paper's main objective is to develop a software tool with integrated algorithms for vibration-based tensile force estimation with a

specific insight for post-tensioned external tendons. Different FE models are developed with different approaches to be used as examples to demonstrate the applicability of TCMS.

4.1. Input Data

A key issue for providing a condition monitoring system is obtaining an accurate measurement of the structural system's objective responses, which reflect the system's objective characteristics. For example, the input parameter of the two mentioned methods for tensile force estimation is their modal responses (i.e., frequencies and modal shapes). Adopted algorithm and methodology for tensile force estimation as pre-determined beam and string theory uses extracted frequencies to model the relationship between frequencies and tensile force. On the other hand, the second approach uses mode shapes for the determination of effective vibrational length. With the determined effective length, the previous methods can be used for tensile force estimation. Therefore, the obtained system responses must be reliable to identify the modal parameters accurately.

To this aim, an emphasis must be put on sensor types, numbers, and arrays. Most of the cables in civil engineering practice have a frequency range between 1 and 50 Hz. Therefore, sensors with the proper range have to be selected. Furthermore, according to the vibration level for either ambient or forced vibration, a proper sensor with a proper dynamic range has to be selected.

4.2. Numerical Models

This study shows the great power of computer-aided tools in engineering practice for computer modeling and computer interface designing. Almost in all researches for computer modeling of tendons, a one-dimensional axially tensioned beam is considered. The tensile force is applied to the beam as a concentrated load from an endpoint. However, modeling a post-tensioned bounded tendon with its main parts like multiple strands embedded in grout inside the duct as a 3D solid model is associated with some challenges. Considering the plasticity and damage behavior [24], complex contact

interaction between wounded wires in strands and internal frictions [25-26], and force distribution in different strands over their wire cross-sections with bending and twisting moment effects are the most critical challenges [27].

For simplification and better force distribution to prevent stress concentration, the model is post-tensioned using temperature analysis. Moreover, the tensile force is applied to a beam with zero mass and without flexural rigidity as a load-bearing part only, while the mass and flexural rigidity are included in a 3D solid part, as shown in Figure (8), which is more manipulatable for meshing and damage definition purposes. The model is applied to temperature differences in two-step as initial and static steps using Equation (9) to apply post-tensioning in the load-bearing part.

$$\alpha = \frac{1}{L} \frac{\Delta l}{\Delta t}$$

$$\Delta l = \alpha l \Delta t \tag{9}$$

$$\varepsilon = \frac{\Delta l}{l}$$

$$T = E \alpha \Delta t A$$

where T is tensile force, E is elastic modulus, α is heat expansion coefficient, Δt is a temperature difference, and A is the cross-sectional area.

An 18.54-meter post-tensioned external tendon is modeled using the software package ABAQUS to validate the applicability of TCMS. All the simulated model data, including experimental in-field frequencies, numerical and analytical frequencies, are reported in detail [22]. A uniformly axially tensioned 2D Euler-Bernoulli beam is also modeled to compare different FE modeling results in this research. In both models, the boundary condition is clamped-clamped in both clear boundaries.

The FE model's frequencies are determined through frequency analysis. However, for experimental modal analysis (EMA) as engineering practice in the real modal identification cases, both 2D and 3D models are also subjected to impact load where the tendon's acceleration response is captured from multiple measurements. The data are recorded from a 20 seconds implicit dynamic analysis.

The acceleration responses are captured as output time histories on eight different locations near the left anchorage zone, as shown in Figure (8). With captured acceleration time histories, the experimental mode shape ratios can be determined and used for tensile force estimation using Method 2.

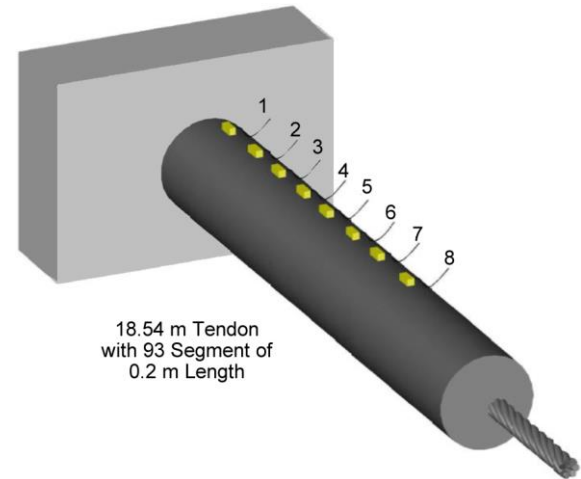


Figure 8. Schematic figure of the 3D Finite Element model.

The frequency values for different models identified through different analyses are shown in Figure (9). The 3D model shows better results in the first five modes, which are the most important modes for tensile force estimation using Method 1, as shown in Figure (9). As the 3D FE model's mode order increases, the corresponding modal frequencies identified through EMA decrease because the modes are excited, but they do not achieve their resonance frequency. At the same time, the identified fundamental frequencies through frequency analysis are too close to the experimental in-field frequencies.

4.3. Verification by Numerical Examples

To ensure that a certain level of accuracy is achieved, the vibrational responses and other parameters of the FE models are used to demonstrate the functionality of TCMS. These vibrational responses, regarded as measured dynamic signals, are used to simulate practical situations where the modal parameters can be identified and used in practical applications. The cable input parameters from a tendon used to model the 3D FE model are presented in Table (1). The 3D FE model is composed of 93 discretized equally-

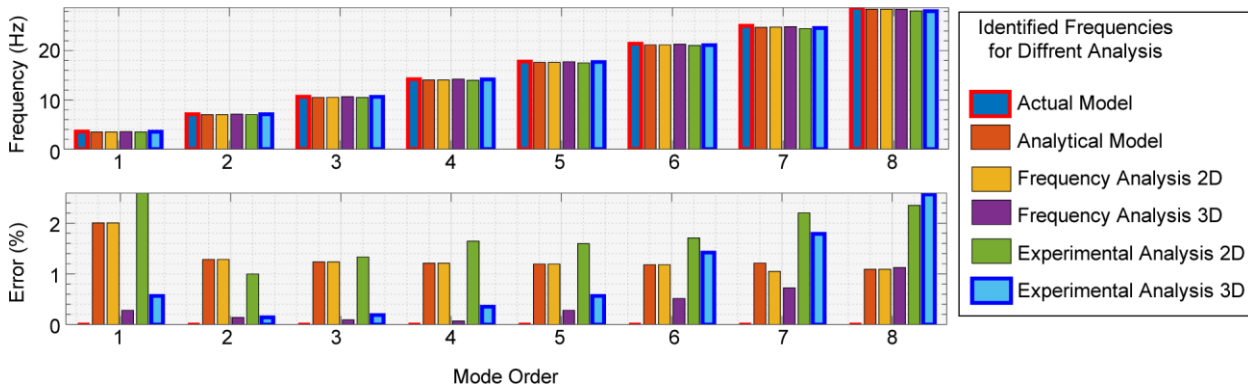


Figure 9. Identified frequencies of the different models with different modal analysis.

Table 1. Tendon modeling input parameters.

Tendon No	Length (m)	Mass Per Unit Length (kg/m)	Flexural Rigidity (kN.m ²)	Tendon Force (kN)
Helmut	18.54	6.125	1.77	100.08

spaced elements. The model is lightly excited with forced vibration as two impulse loads of magnitude 25 and 50 N in the row at a point about 4.6 m of the length from the left end. The nodal accelerations of the model are obtained under impulse loads at a sampling frequency of 50 Hz. Both embedded functions for frequency and mode shape extraction are also validated in the following sections.

4.3.1. Frequencies Extraction Embedded Function

The extracted frequencies for the 3D model

using the PP algorithm are shown in Figure (10). Using the embedded frequency extraction function in TCMS in conjunction with MATLAB built-in functions, the PSDs, as shown in Figure (10), are extracted, where the TCMS and MATLAB results can be compared.

4.3.2. Mode Shape Extraction Embedded Function

All the acceleration responses from the 3D tendon on 92 different locations with equal spaces are recorded to better represent the embedded function's applicability for mode shape determination, as shown in Figure (11). The obtained normalized experimental modal vector for the first four vibrational modes is compared to normalized extracted ABAQUS's mode shapes.

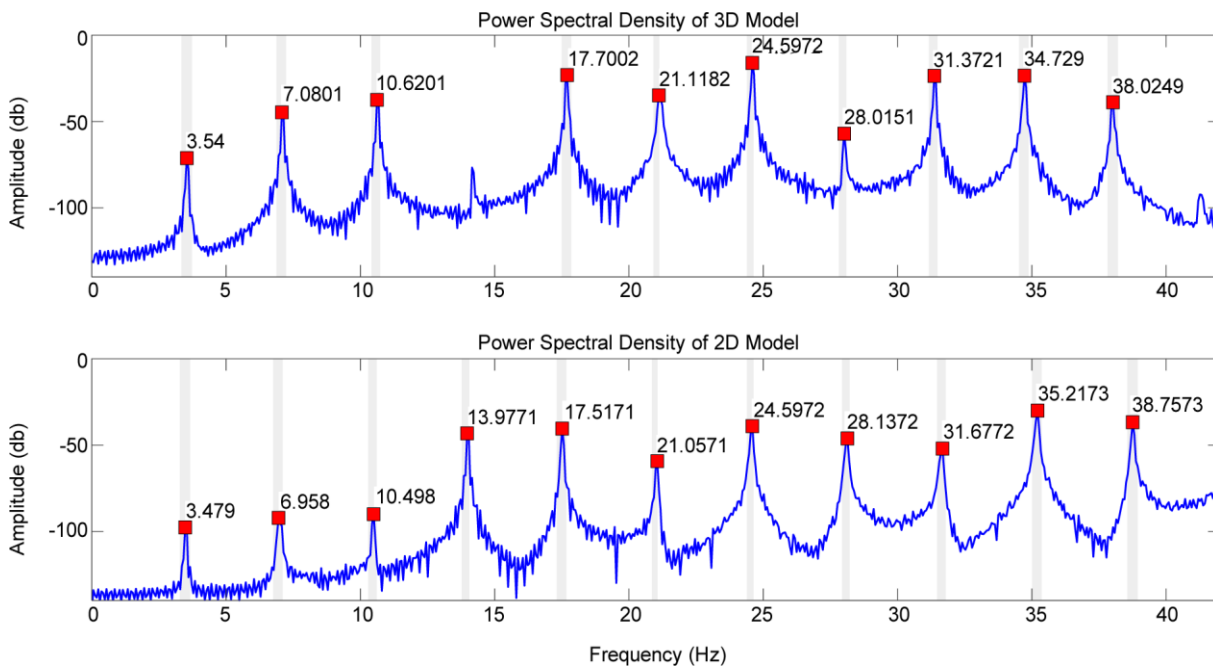


Figure 10. PSDs extracted from MATLAB built-in frequencies extraction function (i.e. pwelch built-in function).

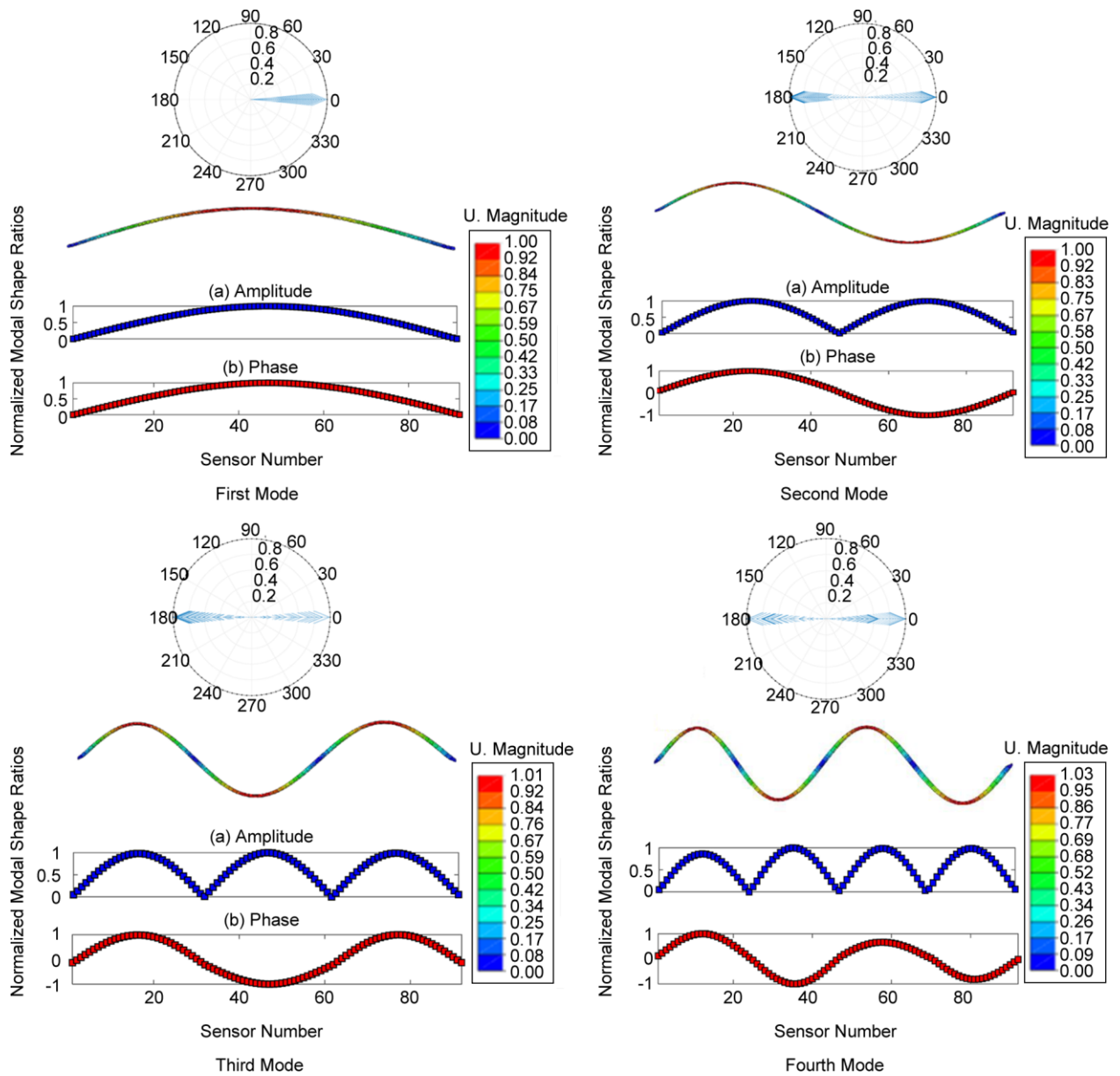


Figure 11. Mode shape ratios for four vibration modes from mode shape extraction function.

The final mode shape vector of each mode by considering the modal amplitude and phase is used as an objective function to determine the effective vibrational length. Therefore, well-distributed mode vectors over tendon length are fully extracted to represent the embedded algorithm's functionality.

5. Results

In order to illustrate the applicability of TCMS, different FE models mentioned in Section 4 are used for tensile force estimation. The results of tensile force estimation can be grouped into two sections based on the applied method. Simple assumptions, like a different number of identified

frequencies, are also considered to compare each method's results.

5.1. Tensile Force Estimation Results (Method 1)

The String theory has been widely used as an analytical formula in earlier works for the tensile force estimation of cables. The major challenge associated with the String theory for tensile force estimation is that the determined frequencies are considered only due to tensile force through the cable. However, the flexural rigidity also causes changes to the frequencies. Therefore, the flexural rigidity effects have been considered a beam with axial tension in a more generalized manner. In this

research, String and Beam's theories are used for comparison by tensile force estimation of FE models mentioned in the previous section with their identified frequencies.

The High-Density Poly Ethylene (HDPE) pipe near the anchorage zone for the tendons causes a high rigidity at both ends, and infill grout inside the duct causes high rigidity along the tendon's length. Therefore, the associated flexural rigidity along tendon length and near both anchorage zones results in higher accuracy for tension estimation using the clamped-clamped beam formula as Equation (4). Besides the tensile force, flexural rigidity is also an important parameter that also can be obtained. To obtain more accurate flexural

rigidity values, the frequency numbers for regression are also essential. More frequency numbers result in better observation and estimation for actual values of flexural rigidity. However, with fault estimation of frequencies, for example, in 2D and 3D models identified with EMA, the flexural stiffness cannot be appropriately identified. The tensile force estimation results with eight identified frequencies and corresponding error values are shown in Figure (12).

The tensile force estimation is conducted with different frequency numbers as set out in the Table (2) to emphasize the SI method's importance for modal frequency identification. With more identified frequencies, both tensile force and flexural

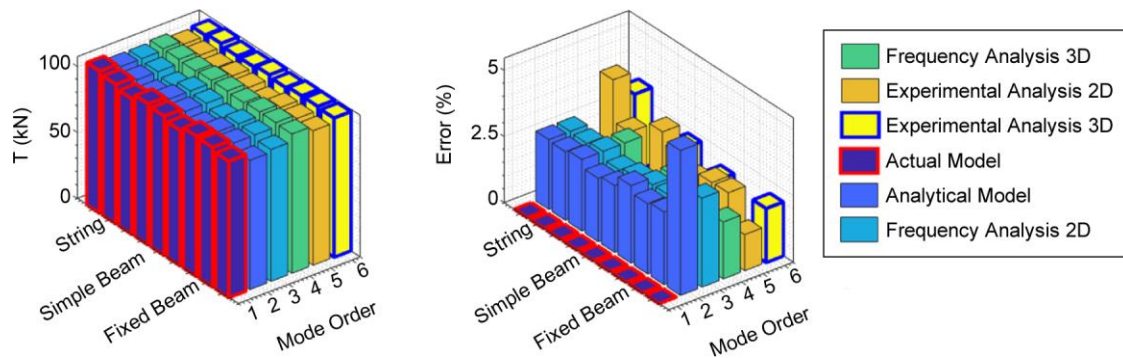


Figure 12. Result of tensile forces for method 1 with the corresponding errors.

Table 2. The results of tensile force estimation for method 1 with 8, 6, and 4 identified frequencies.

Models	String Theory	Beam Theory (Hinged-Hinged)		Beam Theory (Clamped-Clamped)	
	T (kN)	T (kN)	EI (kN/m ²)	T (kN)	EI (kN/m ²)
8 Frequencies					
Actual Model	107.61	105.53	1.68	102.57	1.76
Analytical	104.84	102.86	1.9	99.87	1.85
2D Frequency	104.84	102.86	1.9	99.87	1.85
3D Frequency	106.22	106.1	0.09	105.42	0.094
2D Experimental	103.5	103.06	0.37	101.72	0.27
3D Experimental	104.34	105.89	-1.4	104.32	0
6 Frequencies					
Actual Model	106.73	105.46	1.8	102.5	1.7
Analytical	104.23	102.86	1.91	99.58	1.87
2D Frequency	104.23	102.86	1.91	99.85	1.87
3D Frequency	106.13	106.09	0.13	105.3	0.12
2D Experimental	103.4	102.59	1.12	100.28	1.1
3D Experimental	104.34	106.06	-1.49	104.86	0
4 Frequencies					
Actual Model	106.11	105.68	1.3	103.15	1.28
Analytical	103.36	102.85	1.96	99.79	1.92
2D Frequency	103.36	102.85	1.96	99.79	1.92
3D Frequency	106.13	106.13	0	105.81	0.019
2D Experimental	103.4	103.54	-1.47	102.93	0.005
3D Experimental	105.53	105.93	-1.53	105.52	0

rigidity have higher accuracy. However, if sensors are located in the vicinity of mode blind zones, the corresponding mode frequency is neglected, which results in misalignment in mode order. Therefore, with unequally-spaced mode orders, fitting coefficients outputs are wrong, and the user would not be able to get accurate results. Nevertheless, as it can be concluded from the obtained results set out in the Table (2), method-1 archives almost good accuracy within the 1 to 10% accuracy range.

5.2. Tensile Force Estimation Results (Method 2)

The actual tensile force with high accuracy can be determined by determining the effective vibrational length from multiple mode shape ratios in different modes. Equation (2) with uncoupled variables can be used as a comprehensive formula for all cases with different geometrical and boundary conditions if the length can be modified to effective vibrational length for regression. This method does not require to be evaluated for different geometrical conditions and uncertain boundary constraint effects.

This method has been fully explored for stay cables with different boundary and geometrical conditions in the previous works. In this research, the 3D model as a tendon is evaluated for four major modes with eight acceleration measurements at different locations near the left anchorage end.

With nodal displacement in each mode, the mode shape function vectors are obtained to determine each mode's effective vibration length. A proper sensor array should be adopted to obtain effective vibrational length accurately. A rigorous mathematical foundation is presented for sensor deployment in practical applications of tensile force estimation using mode shape functions [22], where a parametric study is conducted to select the mounting location of sensors optimally. However, in TCMS, the sensor's locations can be manually defined by the user for up to ten sensors. In light of this, the mode shapes can be adequately extracted if the optimal sensor location is considered, as discussed in the aforementioned research regarding sensor deployment that is beyond the scope of this article. In experimental in-filed cases, the proper method to excite more modes is a challenge for

engineering practice. Moreover, noise effects and uncertainty in system identification can challenge the tensile force estimation procedure.

More importantly, the location of the sensors must be chosen appropriately to obtain the best mode shape ratios. The estimated effective vibration length is like the Table (3) for different filter cut-off frequencies. Frequency resolution is also essential for determining mode shape ratios. The frequency sampling rate for determining different mode shape ratios depends on the tendon frequency range. Therefore, one may pay attention to the sampling rate during data acquisition.

By determining the effective vibration length, tensile force estimation can be conducted from the LS tab or sub-tab embedded in the condition monitoring tab as shown in Figure (18) and Figure (20d) with the same geometrical condition. With a proper determination of mode shapes to determine the effective vibrational length, high accuracy within 1 to 2 % can be achieved, as set out in Table (4).

Table 3. The effective vibrational length of the 3D tendon for cut-off frequency 100, 50, and 10 Hz.

Model	Mode 1	Mode 2	Mode 3	Mode 4
3D Experimental				
Cutoff Frequency 100 (Hz)	18.34	18.33	18.33	18.33
Cutoff Frequency 50 (Hz)	18.34	18.33	18.33	18.33
Cutoff Frequency 10 (Hz)	18.34	6.04	10.93	18

Table 4. The results of tensile force estimation for method 2 with 8, 6, and 4 identified frequencies using effective vibrational length.

Model	Beam (Hinged-Hinged)	
	T (kN)	EI (kN/m ²)
8 Frequencies		
Actual Model	103.1	1.67
Analytical	100.55	1.81
2D Frequency	100.55	1.81
3D Frequency	103.71	0.09
2D Operational	100.74	0.36
3D Operational	103.51	-1.35
6 Frequencies		
Actual Model	103.09	1.72
Analytical	100.54	1.82
2D Frequency	100.54	1.82
3D Frequency	103.71	0.12
2D Operational	100.28	1.07
3D Operational	103.54	-1.47
4 Frequencies		
Actual Model	103.3	1.24
Analytical	100.53	1.87
2D Frequency	100.53	1.87
3D Frequency	103.74	0
2D Operational	101.2	-1.4
3D Operational	103.15	0

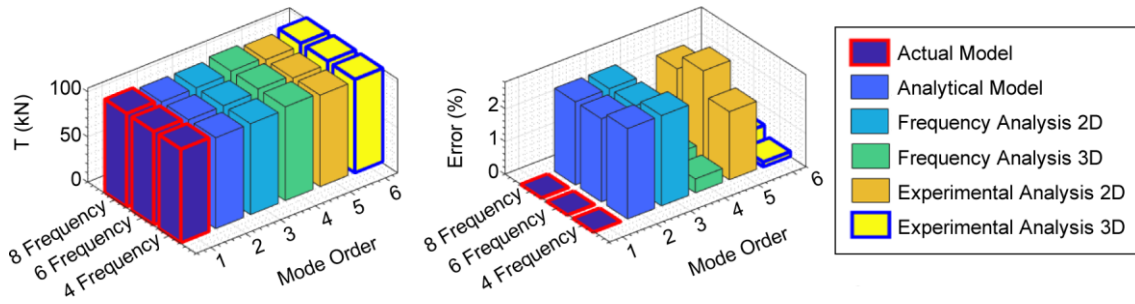


Figure 13. Result of tensile forces for method 2 with the corresponding errors.

Also, the TCMS tackles some other issues associated with the application of this method. It needs to be mentioned that the TCMS allows users to use an adequate number of modes for tensile force estimation. Synchronized measurements can be applied with up to 10 sensors to attain good accuracy. The location of each sensor and its effects on the determination of mode shape vectors can also be thoroughly evaluated. The results of tensile force with corresponding error for eight identified frequencies are shown in Figure (13).

6. Conclusions

An open-source under development software named TCMS for condition monitoring of post-tensioned external tendons is presented. The principal one-dimensional load-carrying nature of cable-like structures like stay cables and strands with different geometrical and boundary conditions also allows TCMS to be used for tensile force estimation of these cables. Therefore, TCMS can also be used with more generalized applicability for other external load-bearing components.

The great power of computer-aided tools is fully exploited in this work. MATLAB has developed its human inelegance interface designing tools for years. Since the 2017 versions, MATLAB has provided the users with App-Designer to develop professional apps with visual components for graphical user interface designing. Unlike, GUIDE environment for GUI designing, App-Designer is provided with an integrated editor where users can quickly program the designed components. Therefore, TCMS is designed on App-Designer because it has many advantages over GUI designing on a code-based or GUIDE environment.

The simulated models of a tendon with different

assumptions, including an axially tensioned beam and a 3D solid model assembled with an axially tensioned beam to model the mass and stiffness, and the load-bearing part, respectively, demonstrated that the 3D proposed model could better represent the actual behavior of the tendon. However, ABAQUS's powerful meshing tools that can be conducted on a solid model make it possible to evaluate different damage effects in a more manipulable manner for future studies. The new modeling approach of tendons shows high accuracy based on a comparison of the frequencies. The frequency values of the proposed model are in an average of less than 1% in the first five modes of vibration.

A comparison between the estimated force results using pre-determined formulas and the mode shape function method shows that a reasonable accuracy can be obtained within a 1 to 10% error for both approaches. However, to obtain more accuracy for the estimated tensile force, the Clamped-Clamped Beam boundary condition for the pre-determined method shows higher accuracy for tendons. The mode shape ratio method also obtains high accuracy within 1 to 2 %.

Condition monitoring of tendons by means of monitoring their most essential features like tensile force and damage occurrence is followed. However, the tensile force cannot be used as a generalized term for investigating force distribution conditions through tendons. Therefore, by detecting the damage locations and their relative intensities, the stress can be a more appropriate term for condition monitoring, which will be fully explored in future versions of TCMS. Other modules for damage detection, data collection, and report generation are aimed to be added in future versions. In a technical

aspect, a variety of methods can also be added to detect closely spaced modes, force estimation of unsymmetric load-bearing components, etc.

7. Data and Resources

The acceleration response data as 8 and 92 channels of data and the source code of TCMS are available on Git-Hub from the following link: Response data. The commercial software package MATLAB is from the Mathworks website <http://www.mathwork.com>. In addition, the App-Designer GUI designing tool is accessible as an internal module on MATLAB. The current version of TCMS has been designed on MATLAB 2019b version, and it is a 64-bit application for Windows operating system.

8. Appendix A (GUI)

In this section, different GUI tabs developed for each algorithm are presented. The data presented in each section are from the 3D proposed FE tendon, as explained in Section 4.2. The following sections are explained in summary based on the developed section as previously presented in the main body of the paper.

8.1. Filter Parameter Selection

The first tab allows the user to select the desired data cleaning parameters as a Butterworth filter to observe the data cleaning better. The channel's data are added as an input to the software, and then the

user can select the channel number from a pop-up menu to only show the selected channel data output on display UI figures. Figure (14) shows the selected channel raw data, and the filtered data are plotted simultaneously with different knobs to specify the filter order and cut-off frequency values for different filters. Moreover, to have a better signal observation in frequency and time domain for both raw and filtered data, the FFT spectrum and signal waveform are displayed in this tab simultaneously. The filter selection module is only aimed to help the user as an individual tab for filter parameters selection based on the observation of raw data in the time and frequency domain simultaneously. The altering of the different parameters results can be observed in the frequency domain, as shown in Figure (14). It needs to be mentioned that the changes of the parameters are not applied on the data channels and are only aimed to be used for better parameters selection. However, the data cleaning tab is also provided for the user to apply both filtering and baseline correction with selected and evaluated parameters in the first tab. The user can apply changes in all the data channels as an engineering tool, as shown in Figure (15).

8.2. Data Cleaning

The user can apply the filtering on all the data channels with parameters selected based on the previous section. Velocity and displacement responses

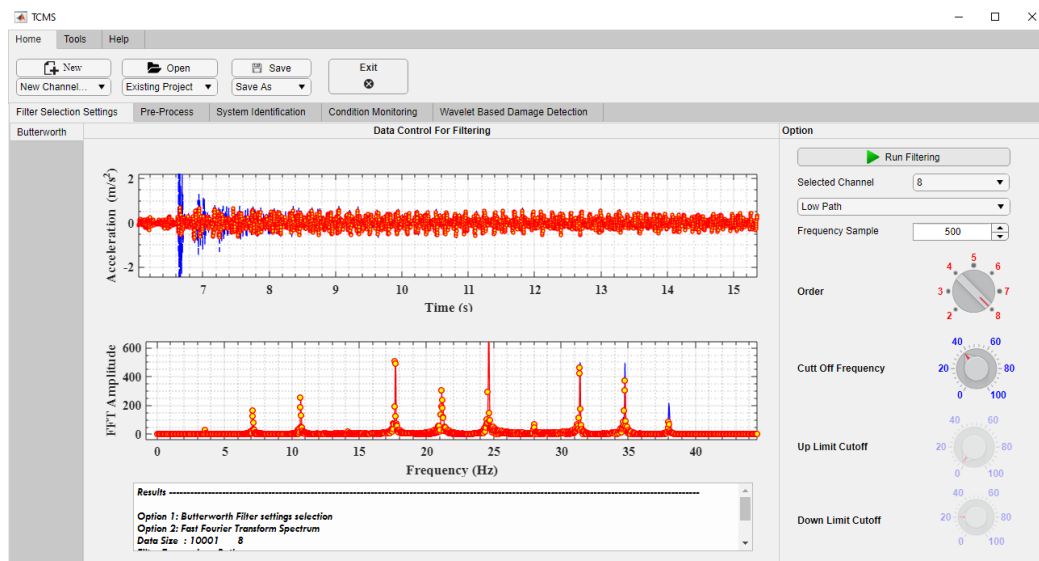


Figure 14. Filter parameters selection tab.

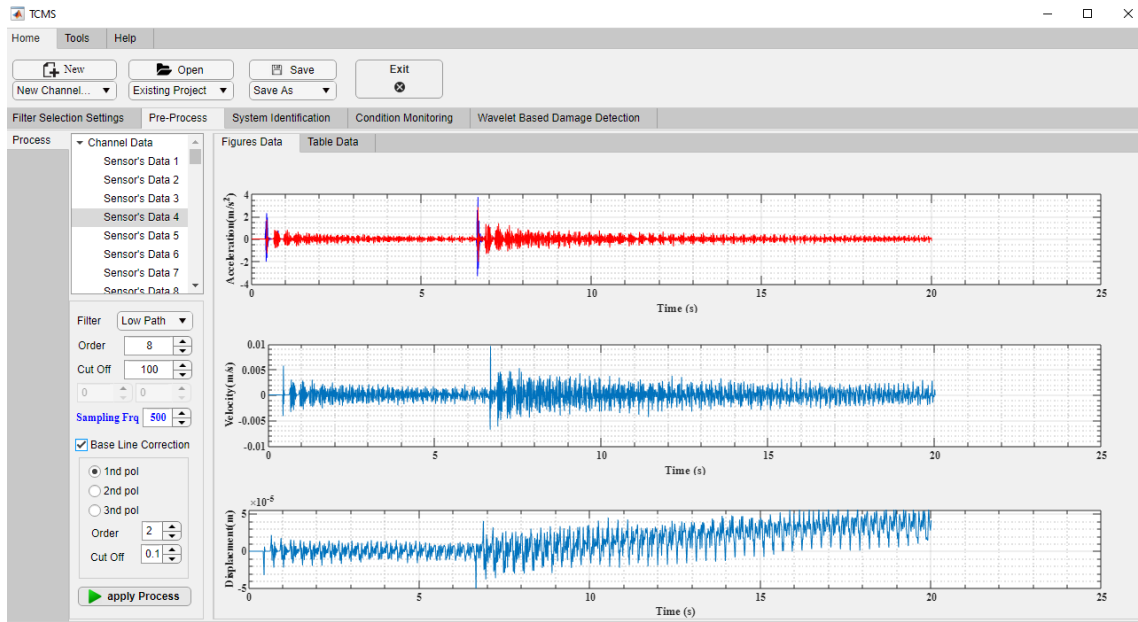


Figure 15. Data correction tab.

are also calculated and shown on the embedded figures to observe signals in the time domain better, as shown in Figure (15). Then, all the data, including the raw and filtered data, are added to the embedded table. Also, the displacement and velocity data are added in table data, where the user can save the data for added options in a pop-up menu.

The baseline correction as an optional checkbox can be selected. Moreover, some options are added for selecting the order of the polynomial, high pass Butterworth filter order, and cut-off frequency where they are up to be selected by the user.

8.3. System Identification

The sampling frequency, the length of the sliding window, and the value of overlap of each window should be inserted by the user. The user can select the window function as three options: Hamming, Hanning and rectangular window types, as shown in Figure (16) from the radio button panel. MATLAB built-in function as a select peak function is used with two options: minimum peak distance and minimum height distance to automatically make the frequency identification, as shown in Figure (16b). Also, a manual tab is added when the user wants to add the data manually, as shown in Figure (16a).

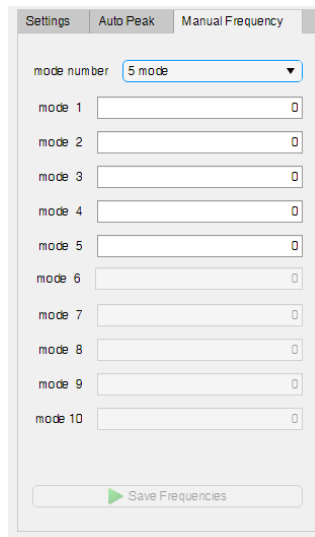
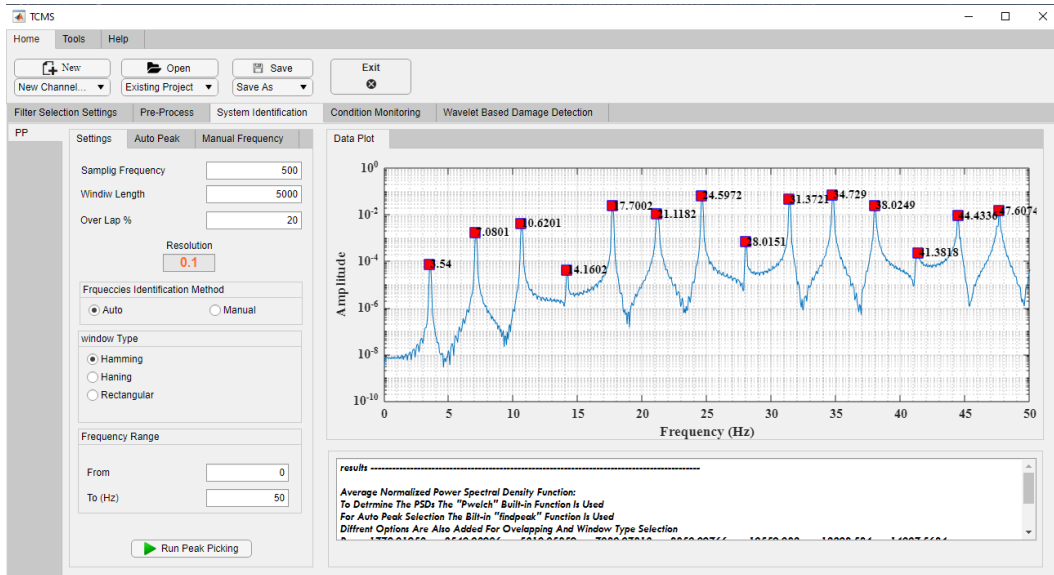
8.4. Initial Frequency Range Estimation

With the initial design information reported as initial geometrical and structural data like mass per unit length, length, and EI values, the frequency range can be determined using pre-determined formulas mentioned in Section 3.3. The user first specifies the initial geometrical values, then a range for EI and tensile force can also be defined. The first twenty modes are displayed in the frequencies tab group by selecting the desired formula from the tree on the tab's left side, as shown in Figure (17). Also, to better observe the effects of EI and tensile force changes on frequency values, two scroll bars can be used in this tab.

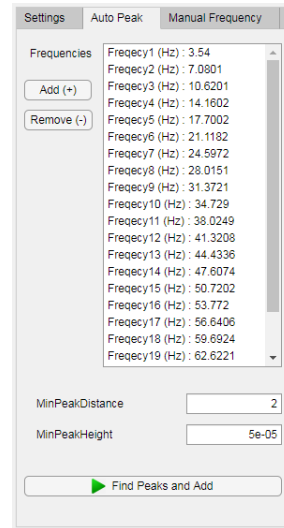
8.5. Tensile Force Estimation

This tab uses generated functions from MATLAB's curve fitting toolbox as a custom equation option, which uses the non-linear LS algorithm. Three main functions for TCMS are used as String, Simple Beam, and Fixed Beam functions. All the outputs for fit-result are also shown in a text area in TCMS, as shown in Figure (18).

The pre-determined formula and the objective function for regression can be selected by users as three options, as shown on the left tree of the Figure (18). The initial values for regression and geometrical information like length and mass per unit length also need to be specified.



(a) Manual Frequencies Nested Tab



(b) Auto Frequencies Nested Tab

Figure 16. System Identification main tab.

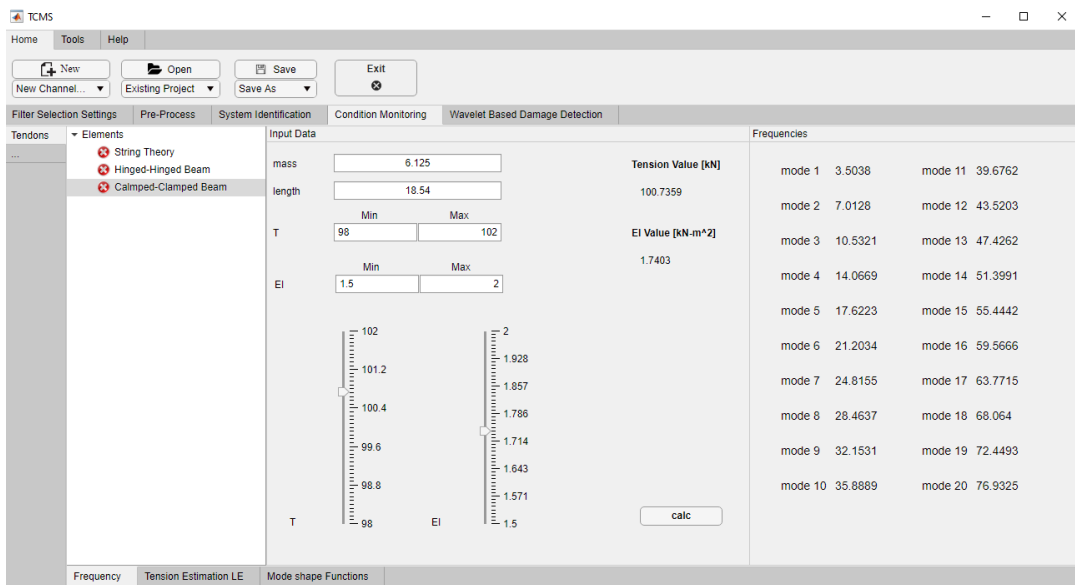


Figure 17. Frequencies estimation tab using initial values with a determined range of tensile force and EI.

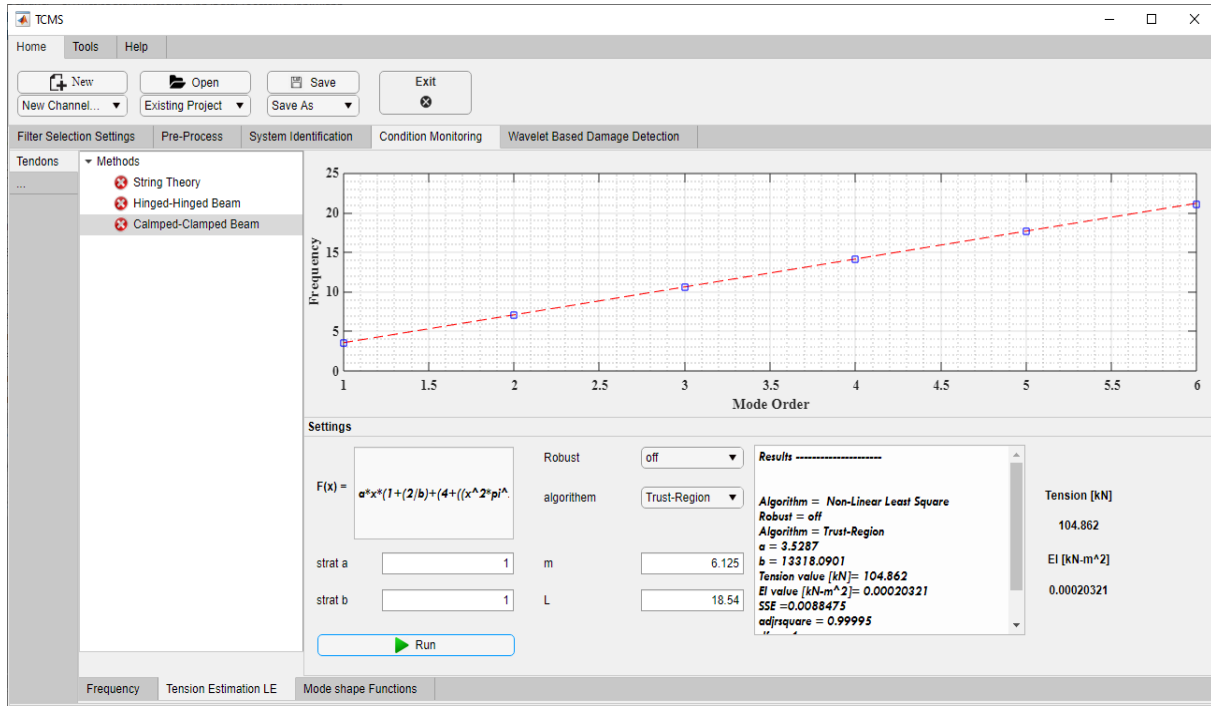


Figure 18. Tensile force estimation tab using pre-determined formulas.

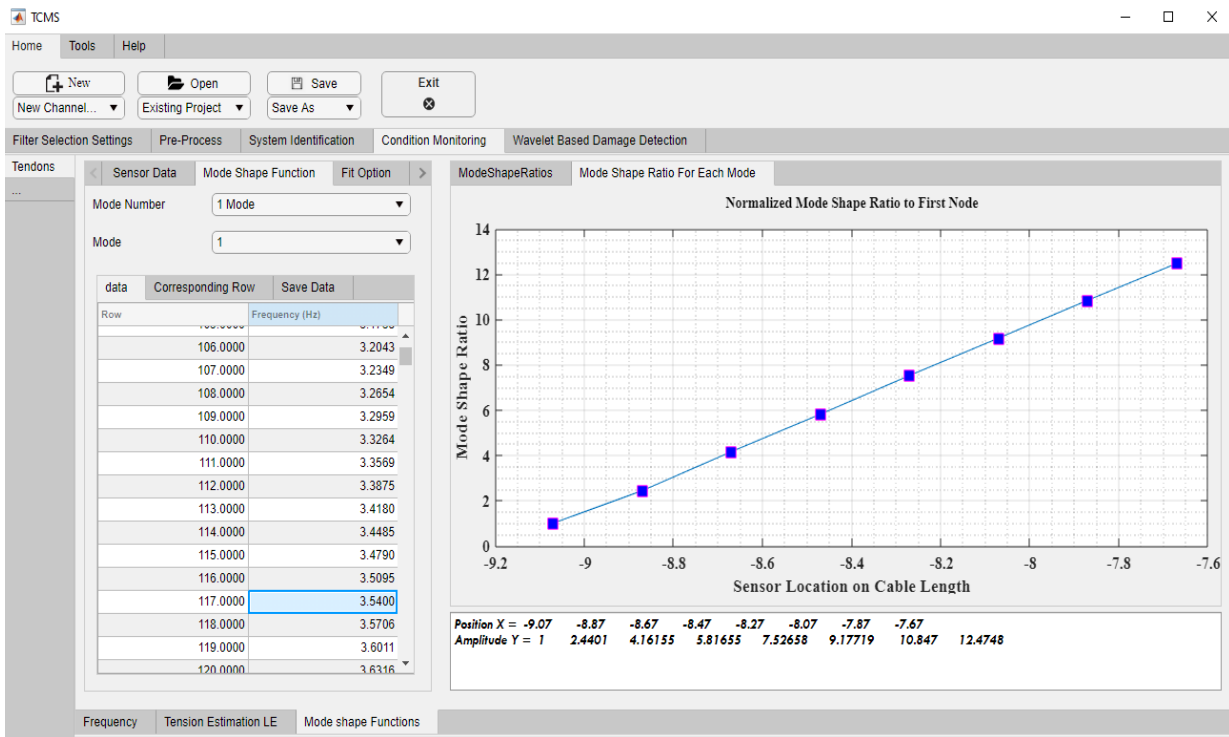


Figure 19. Tensile force estimation tab using mode shape functions from multiple measurements.

Finally, the regression result and determined tensile force and the EI values are also presented.

By inserting the sensor's locations and data as shown in Figure (19), the user can obtain the effective vibrational length of each mode. After

determining effective vibrational length, a subtab, as shown in Figure (20), is embedded in TCMS to estimate the tensile force from determined coefficients using the LS algorithm. However, the user also can use the tensile force estimation main tab as Section 3.4.2.

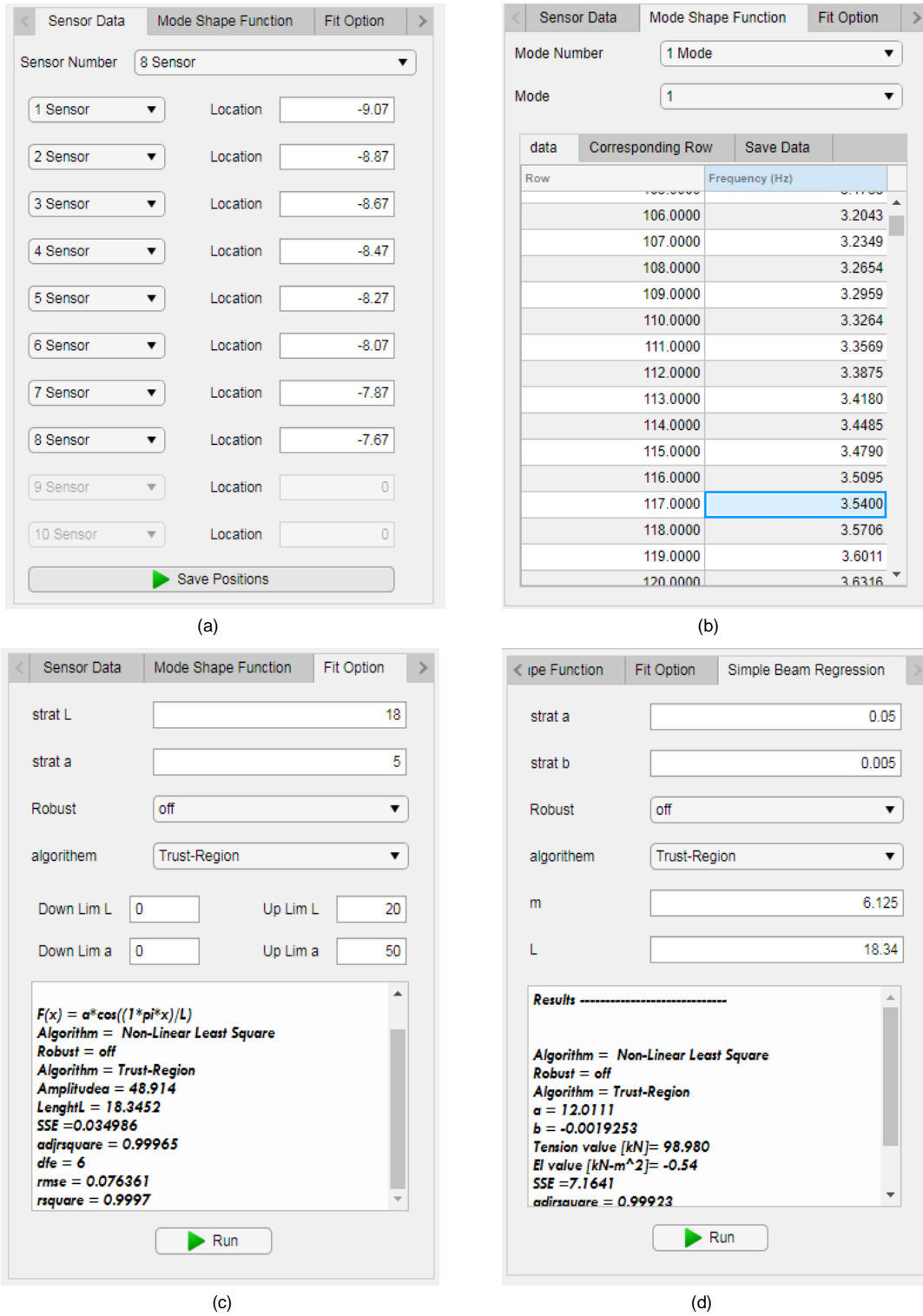


Figure 20. Mode shape functions method nested tabs; (a) Sensor locations; (b) Vibration mode information; (c) Curve fitting options for effective vibration length determination; and (d) Curve fitting options for tensile force estimation, according to Equation (5).

9. Acknowledgment

This study is part of the research project No. 7166, Structural Health Monitoring of Pre-stressed Concrete Bridges, funded by the IIEES. This support is greatly acknowledged.

10. Conflict of Interest

The authors declare that they have no known competing financial interests or personal relationships that could have influenced the work reported in this paper.

References

1. Li, D., Zhou, Z., and Ou, J. (2011) Development and sensing properties study of FRP-FBG smart stay cable for bridge health monitoring applications. *Measurement*, **44**(4), 722-729.
2. Duan, Y.F., Zhang, R., Zhao, Y., Wing Or, S., Fan, K.Q., and Tang, Z.F. (2012) Steel stress monitoring sensor based on elasto-magnetic effect and using magneto-electric laminated composite. *Journal of Applied Physics*, **111**(7), 07E516.
3. Wenzel, H. and Furtner, P. (2006) Damage detection and bridge classification by ambient vibration monitoring-application of Brimos at Two stay cable bridges in China. *Proceedings of the 4th China-Japan-US Symposium on Structural Control and Monitoring*.
4. Casas, J.R. (1994) A combined method for measuring cable forces: the cable-stayed Alamillo Bridge, Spain. *Structural Engineering International*, **4**(4), 235-240.
5. Mehrabi, A.B. and Tabatabai, H. (1998) Unified finite difference formulation for free vibration of cables. *Journal of Structural Engineering*, **124**(11), 1313-1322.
6. Russell, J.C. and Lardner, T.J. (1998) Experimental determination of frequencies and tension for elastic cables. *Journal of Engineering Mechanics*, **124**(10), 1067-1072.
7. Fang, Z. and Wang, J.Q. (2012) Practical formula for cable tension estimation by vibration method. *Journal of Bridge Engineering*, **17**(1), 161-164.
8. Sagüés, A.A., Kranc, S.C., and Hoehne, R.H. (2000) *Initial Development of Methods for Assessing Condition of Post-Tensioned Tendons of Segmental Bridges* (No. Final Report).
9. Sagüés, A.A., Cotrim, C., and Balakrishna, V. (2005) *Vibrational Evaluation of Tendons in Segmental Sections of Sunshine Skyway Bridge Main Spans* (No. BD544-03).
10. Sagüés, A.A., Kranc, S.C., and Eason, T.G. (2006) Vibrational tension measurement of external tendons in segmental post-tensioned bridges. *Journal of Bridge Engineering*, **11**(5), 582-589.
11. Lee, J.K. and Kang, J.W. (2019) Experimental evaluation of vibration response of external post-tensioned tendons with corrosion. *KSCE Journal of Civil Engineering*, **23**(6), 2561-2572.
12. Kim, B.H., Park, T., Shin, H. and Yoon, T.Y. (2007) A comparative study of the tension estimation methods for cable supported bridges. *International Journal of Steel Structures*, **7**(1), 77-84.
13. Chen, C.C., Wu, W.H., Huang, C.H., and Lai, G. (2013) Determination of stay cable force based on effective vibration length accurately estimated from multiple measurements. *Smart Structures and Systems*, **11**(4), 411-433.
14. Chen, C.C., Wu, W.H., Leu, M.R., and Lai, G. (2016) Tension determination of stay cable or external tendon with complicated constraints using multiple vibration measurements. *Measurement*, **86**, 182-195.
15. Wu, W.H., Chen, C.C., Chen, Y.C., Lai, G., and Huang, C.M. (2018) Tension determination for suspenders of arch bridge based on multiple vibration measurements concentrated at one end. *Measurement*, **123**, 254-269.
16. Chen, C.C., Wu, W.H., Chen, S.Y., and Lai, G. (2018) A novel tension estimation approach for elastic cables by elimination of complex boundary condition effects employing mode shape functions. *Engineering Structures*, **166**, 152-166.
17. Farrar, C.R. and Worden, K. (2012) *Structural Health Monitoring: a Machine Learning Perspective*. John Wiley & Sons.
18. Butterworth, S. (1930) On the theory of filter amplifiers. *Wireless Engineer*, **7**(6), 536-541.
19. Chiu, H.C. (1997) Stable baseline correction of digital strong-motion data. *Bulletin of the Seismological Society of America*, **87**(4), 932-944.
20. Felber, A.J. (1993) *Development of a Hybrid Bridge Evaluation System*. Ph.D. Thesis Department of Civil Engineering. University of British Columbia, Vancouver, Canada.
21. Welch, P. (1967) The use of fast Fourier transform for the estimation of power spectra: a method based on time averaging over short, modified periodograms. *IEEE Transactions on Audio and Electroacoustics*, **15**(2), 70-73.
22. Wenzel, H. and Pichler, D. (2005) *Ambient Vibration Monitoring*. John Wiley.

23. Geier, R., De Roeck, G., and Flesch, R. (2006) Accurate cable force determination using ambient vibration measurements. *Structure and Infrastructure Engineering*, **2**(1), 43-52.
24. Yapar, O., Basu, P.K. and Nordendale, N. (2015) Accurate finite element modeling of pretensioned prestressed concrete beams. *Engineering Structures*, **101**, 163-178.
25. Zhang, D. and Ostoja-Starzewski, M. (2016) Finite element solutions to the bending stiffness of a single-layered helically wound cable with internal friction. *Journal of Applied Mechanics*, **83**(3).
26. Stanova, E., Fedorko, G., Kmet, S., Molnar, V., and Fabian, M. (2015) Finite element analysis of spiral strands with different shapes subjected to axial loads. *Advances in Engineering Software*, **83**, 45-58.
27. Machida, S. and Durelli, A.J. (1973) Response of a strand to axial and torsional displacements. *Journal of Mechanical Engineering Science*, **15**(4), 241-2.